machines

MDPI

*Article*

# Effect of Hardening Temperature on Maraging Steel Samples Prepared by Direct Metal Laser Sintering Process

**Radoslav Vandzura *, Vladimir Simkulet, Matus Gelatko, Michal Hatala and Zuzana Mitalova**

Faculty of Manufacturing Technologies, Technical University of Košice, 080 01 Prešov, Slovakia
* Correspondence: radoslav.vandzura@tuke.sk; Tel.: +421-55-602-6359

**Abstract:** This paper deals with the application of the direct metal laser sintering (DMLS) process, which already has a dominant position in the area of additive manufacturing (AM). This DMLS technology is used in many branches of industry and medicine, especially in piece production, small series, and prototypes. The portfolio of used metal powder materials includes aluminum alloys, austenitic steels, maraging steels, special alloys of nickel and titanium. The properties of these products are very often improved by further heat treatment after printing, such as a hardening process, by which microstructure and hardness can be increased. Heat treatment processes of metal AM components are already described, but experiments focused on optimization of these processes are still missing. In the article, the maraging steel samples printed by the DMLS method are subjected to testing after hardening processes, which differ by reducing the maintaining time at a defined temperature, recommended by the manufacturer. The result of the evaluation will be the reaching of similar results, which are set by the powder manufacturer, however, with shorter time of samples treatment. Therefore, the elevated temperature is selected, with the purpose of monitoring the shortest possible time of a temperature impact. The experimental temperature was set 590 °C with different durations at this temperature, for 1, 2, 3, 4, 5 and 6 h. The cooling process runs controlled in the furnace or in the still air. The maintaining time proved to be the most ideal already at 1 h exposure and cooled in the still air, where a higher hardness value of around 50 HRC was reached. During the resulting microstructure evaluations, fine carbids and martensitic lamellae were observed. More uniform and finer lamellar microstructure occurred at 5 and 6 h temperature intervals.

**Keywords:** maraging steel; printing; laser; sintering; hardening; hardness; microstructure



**Citation:** Vandzura, R.; Simkulet, V.; Gelatko, M.; Hatala, M.; Mitalova, Z. Effect of Hardening Temperature on Maraging Steel Samples Prepared by Direct Metal Laser Sintering Process. *Machines* **2023**, *11*, 351. https://doi.org/10.3390/machines11030351

Academic Editor: Mark J. Jackson

Received: 18 January 2023
Revised: 19 February 2023
Accepted: 25 February 2023
Published: 3 March 2023



## 1. Introduction

The direct metal laser sintering (DMLS) 3D printing method and other comparable printing techniques, such as Selective Laser Sintering (SLS) and Laser Powder Bed Fusion (LPBF), have already found use in a variety of technical fields, as well as in the medical field, aerospace industry, and other fields [1–3]. In addition to polymers, other materials can be used, including iron, non-ferrous metals, ceramics, and composites. [4–10]. By adding additive elements to the alloy [4–8], which is regularly experimented with in addition to finishing operations like heat treatment and hardening [2,5,7–11], the qualities of the material are improved. In the field of fast prototyping, the DMLS and SLS processes have their origins in the 1970s with the creation of prototypes. [1–6,8–11].

Due to the benefits they provide, particularly the more effective fabrication of components with extremely complicated geometries, interest in these technologies of additive manufacturing of metal parts has increased significantly over the past several years. Over the past ten years, a small number of businesses have begun to create DMLS technique variants with the intention of advancing process technology in general [12]. Figure 1 illustrates the evolution of DMLS through the year 2004 together with other related technologies by showcasing innovations and commercial developments in chronological order on the vertical axis and technological area on the horizontal axis.

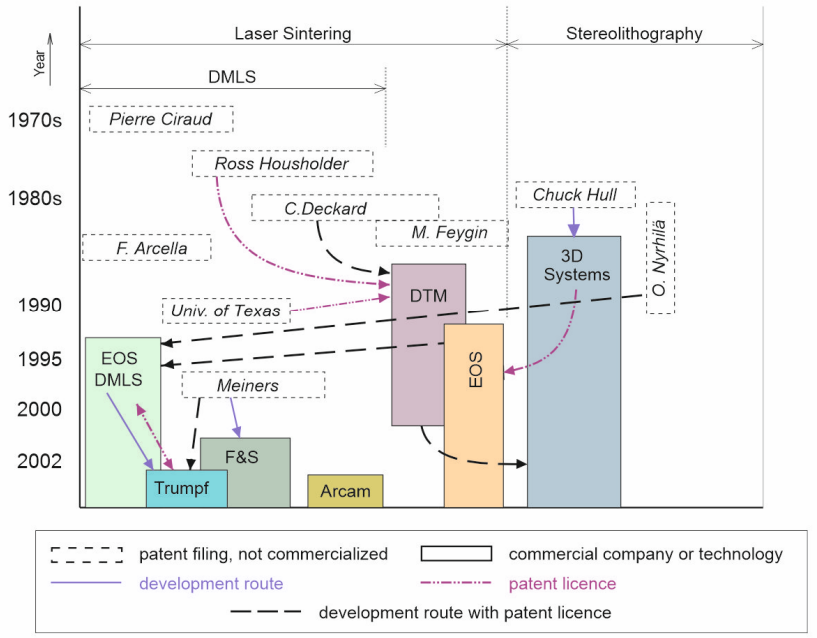


**Figure 1.** DMLS development and patent history since 1970.

A decade before additive manufacturing techniques and the name Rapid Prototyping became popularized in the 1960s of the 20th century, the notion of fabricating metal components via the laser-induced fusing of powder material was first proposed by Frenchman Pierre Ciraud [12,13]. His fundamental concept is to enable the production of parts without the need for casting molds. This idea was not sufficiently ready for commercialization, because computers were then only in their infancy. Six years after Ciraud, another inventor named Ross Householder submitted his patent application. He described a system and technique that were similar to subsequent commercial laser sintering systems [12,14].

The invention's claimed goal was to develop a novel molding method for building up three-dimensional components, using layers that could be controlled by computer technology. In one design, the layers are created using fusible particles, which are then individually fused by a laser beam to define the final result. Housholder was only able to thoroughly test a variant approach that did not require a laser at the time due to the prohibitively expensive cost of lasers at the time. His creation was not commercialized at the time and went unnoticed until DTM Corporation came upon it, while working on their own patent filings. [12,15].

Early through the 1980s, the initial steps in the commercialization of additive manufacturing techniques and powder-based additive processes were taken. Chuck Hull, the creator of 3D Systems and the US 4,575,330 patent [16], launched commercial "RP" in August 1984. In the area of laser sintering, EOS acquired exclusive rights to the full 3D system patent portfolio in 1997. Around 1986, Hull's approach was the subject of research by master's candidate Carl Deckard at the University of Texas (UT), who used powdered materials instead of liquid ones. Part Generation by Layerwise Selective Sintering (PGLSS) was the original name of his technique; Selective Laser Sintering was eventually used (SLS). A computer-aided laser apparatus that sequentially sinters a number of powder layers to create a desired portion layer-by-layer, was the subject of the ensuing October 1986 patent application [12,17].

In April 1987, Helisys was founded by Michael Feygin to commercialize his ideas, where he used a scanning laser in the production of laminated molds. Another similar development to cast shapes without the use of a mold took place by Frank Arcello, in March 1988. As a consequence of research and development by Deckard, Beaman, and associates at UT, DTM Corp. launched Sinterstation 2000 as the first commercially available system for laser sintering in December 1992. By EOS GmbH of Munich, Germany, the

second industrial laser sintering system was introduced in April 1994. The combination of powder metallurgy technology from Electrolux Rapid Development (ERD) by Mr. Russia from Finland, and EOS plastic laser sintering technology led to the creation of the first commercial DMLS system.

A revolutionary powder idea for pressureless sintering with extremely little shrinkage was created by Nyrhilä in 1989 [18]. Before successfully reaching an agreement on a patent license and collaboration between ERD and EOS in 1994, he had the notion of employing this technique for DMLS and had discussed it with a number of possible partners. In 1994, the installation of the first test systems created by EOS [12], where the modified bronze nickel-based powder was sintered in 100 µm layers using a 100W CO2 laser, was done and commercial EO-SINT M 250 systems were deployed for another year. This opened the door for the first really commercial application of DMLS for quick machining and made it feasible to make complicated components with high accuracy and acceptable surface quality, which was previously impossible with any other direct metal technique. Since then, despite several changes in ERD's owners, the relationship remained. A German cooperative initiative was launched at the end of 1995 to improve the DMLS process further and make it possible to produce fully dense components by fully melting single component ceramic and metallic materials like 1.4404 steel [12].

Within the German cooperative project, at the end of 1995, together with partners EOS, Fockele and Schwarze (F&S) and Fraunhofer Institutes, developed equipment for the construction of fully dense parts from one-component ceramic and metal materials, using DMLS technology.

Due to the small market size and prospects for machinery sales, the Trumpf company terminated PBF between 2006 and 2014 [13]. In 2002, f. Arcam invented the technique for electron beam powder bed fusion and unveiled the first industrial system. In parallel with Arcam, the Extrude Hone Company unveiled the first AM system based on metal sintering in 1999 [15].

Systems from traditional machine makers, such as Trumpf and DMG, followed suit during the following two decades. (Figure 2.) The first business to adopt a traditional plasma arc welding procedure for AM machine technology was Norsk Titanium in 2007. The aerospace industry was the major area of attention. HP and Desktop Metal introduced their metal printer technologies in 2016 [15], entering the market.

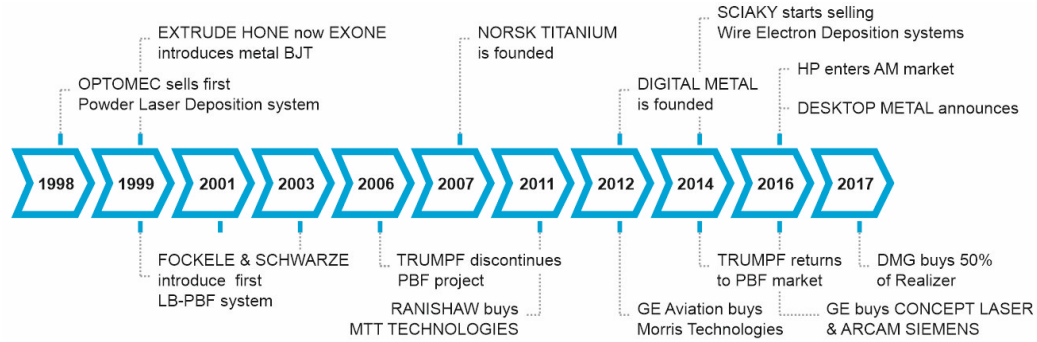


**Figure 2.** Summarized development of DMLS history after 2004 [15].

Other operations, including as the curing process, enhance the final qualities of the objects produced by these printers. Some researchers [19–21] studied the mechanical characteristics of powder additive products and noted alterations in the material's properties or microstructures after the printing process or after the operation was finished [22,23].

According to several publications [7–9,24–29], these qualities have recently been enhanced by heat treatment procedures (such as tempering, annealing, hardening, etc.), where the values of hardness and strength have more than doubled. Another of the researched features, that is a part of other essential usable properties of the product generated by

this method of 3D printing technology, is the fatigue strength of the material, prepared by DMLS or a similar employed laser melting technique [30,31].

The heat treatment, annealing for example, demonstrably changes mechanical properties of AM materials in the study: Production of Hybrid Joints by Selective Laser Melting of Maraging Tool Steel 1.2709 on Conventionally Produced Parts of the Same Steel, by K. Kucerová, et. al, where hybrid parts were made by DMLS technology, from maraging steels 18Ni300 (MS1) and VACO180. A study deals with various ways of annealing and cooling of mentioned hybrid material, and the influence of these process on mechanical properties of the material, is taken into account. Original tensile strength was 1029 MPa in components. Using the solution annealing, yield strength was decreased by 150 MPa. In the case of precipitation annealing, a strength increased to 2011 MPa [24].

During the experiment by Luca Fachini, et. al: Ductility of a Ti-6Al-4V alloy produced by selective laser melting of pre-alloyed powders, martensitic structure was stabilized, due to the process variation, which consequently led to the increasing of mechanical properties of Ti-6Al-4V alloy [7]. Some other researches are focused on the resulting mechanical properties of the material, reached by the input AM process parameters variation, however, not by the material properties changing after the 3D printing process. There are not too many available sources and scientific studies, which are aimed on the MS1 material properties variation, or any similar maraging steels, prepared by the AM process. Experiments on conventionally made maraging steel materials, could be the good stepping-stones, such as studies [32,33]. Nevertheless, these materials includes apparently the same chemical compositions, a different manufacturing method need to be taken into account, which refers to AM materials prepared using the PBF technologies. Available AM materials generally have one heat treatment process, in order to increase properties of individual material. However, it is appropriate to pay attention on researches, focused on various heat treatments, with the aim to recognize the behavior of material, its mechanical properties and inner structure changes at different ways and conditions of heat treatment.

Evaluated material reaches double values of hardness and strength increase, after the heat treatment with 490 °C temperature for 5 h. Examined lower temperature did not reach such an effect [20,21,24,28]. Therefore, the plan of the experiment will be the reaching of similar results and evaluate the best possible time of elevated temperature impact on the sample, using the epistemological process.

## 2. Materials and Methods

Direct metal laser sintering (DMLS) means sintering using a laser beam, where metal powder is directly used to produce metal connections in the construction process. A diverse portfolio of materials used in the production of metal parts by DMLS, developed by EOS GmbH, as the first commercial method of rapid prototyping [1–3,6,8], includes Tool Steels, Stainless Steels and Maraging Steels, various Nickel Alloys, Titanium, Refractory Metals, light metals as Aluminum, Copper etc. [1–5,8].

Direct metal laser sintering (DMLS), electron beam melting (EBM), selective heat sintering (SHS), selective laser melting (SLM) and selective laser sintering (SLS) are some of the most popular printing methods utilized in the Powder Bed Fusion process (PBF), according to ISO / ASTM 52900:2021 standard. Laser or electron beams are used in powder bed fusion (PBF) techniques to melt and fuse separate material powder particles. The powder material must be dispersed over earlier layers in every PBF procedure. This can be accomplished using a variety of devices, such as a roller or a blade. The supply of new materials is provided by a hopper or reservoir beside the bed. The same process as selective laser sintering (SLS), direct metal laser sintering (DMLS) uses metals rather than polymers. Layer-by-layer, the powder is sintered during the process. The basic principle of PBF technology is shown in Figure 3 [34–36].

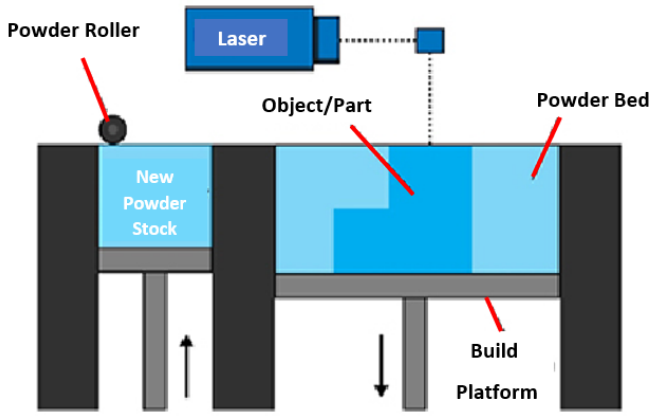


**Figure 3.** Principle of PBF and other similar technologies [36].

Advantage of DMLS process in comparison other similar methods (such as SLS, LPBF and more), that it provides higher resolution of a details, thanks to the use of thinner layers, which allows a smaller diameter of powder particles. This ability makes it possible to create more complex parts of shapes [3,4], which are also used in the field of comfort cooling and small structural components with specific shapes. Heat treatment of these printed products could optimize and improve their properties [4,6–8,13]. The manufacturer recommends a prescribed temperature of 490 °C for 6 h during the curing process.

The experiment is based on a heat treatment (age hardening) of MS1 material samples, for 1–6 h at the increased hardening temperature equal to 590 °C. The main aim of the experiment is to evaluate the variation of hardness and microstructure within the MS1 material at the various durations of hardening process at a certain temperature. Concretely, at a 590 °C for 1, 2, 3, 4, 5 and 6 h. Additionally, final structure and hardness were evaluated after the cooling influence, as for the cooling in the still air, so for the cooling in the furnace. Heat treatment conditions for different material samples are summarized in Table 1.

**Table 1.** Conditions of experimental heat treatment process.

| Sample | Heat Treatment | | |
|---|---|---|---|
| | Duration Time (Hours) | Curing Temperature (°C) | Cooling |
| 1.0 | 1 | 590 | in the still air |
| 2.0 | 2 | 590 | in the still air |
| 2.1 | 2 | 590 | in furnace |
| 3.0 | 3 | 590 | in the still air |
| 4.0 | 4 | 590 | in the still air |
| 5.0 | 5 | 590 | in the still air |
| 6.0 | 6 | 590 | in the still air |
| 6.1 | 6 | 590 | in furnace |

– furnace temperature is raised to curing temperature in 30 min.

For investigated experiment, maraging steel made by the DMLS production method, was chosen, marked by the manufacturing company as MS1. This powder material is optimized for the application in EOSINT company 3D printing systems.

A metal powder of this maraging steel with a particle diameter from 20 to 80 µm was used, which was bonded without the need of a binder, using a high-power laser beam [1–8].

EOS Maraging Steel MS1 powder material corresponds to the American classification: 18% Ni Maraging 300, EU standard norm 1.2709, and German norm classification X3NiCoMoTi 18-9-5 [37]. This material can be easily heat-treated, using the heat hardening process, which provides excellent hardness and strength [38]. The chemical composition of tested material [37–39] is shown in Table 2.

**Table 2.** Chemical composition of investigated material.

| Element * | Al | Ti | Mn, Si | Cr, Cu | Mo | Co | Ni |
|---|---|---|---|---|---|---|---|
| Mass (%) | 0.05<br>–<br>0.15 | 0.6<br>–<br>0.8 | up<br>to<br>0.1 | up<br>to<br>0.5 | 4.5<br>–<br>5.2 | 8.5<br>–<br>9.5 | 17<br>–<br>19 |

* C is below 0.03 percent, P and S is below 0.01 percent, Fe makes up the rest.

Components or semi-components printed in this way manufactured of maraging steel on the printer from EOS are easy to machine after the build process and can be very easy to improve after finishing operations such as hardening. In their research papers, various authors describe the improvement of properties by curing at 490 °C for 6 h [20,28,29], where they reached an almost twice as high strength and hardness value. For our experiment, we will use a higher temperature and a shorter dwell time on the component to achieve a similar effect. The mechanical properties reporting by manufacturer [38,39], are listed in Tables 3 and 4.

**Table 3.** Mechanical Properties as built (a) and printed and also hardened (b).

| Density ρ, (g/cm$^3$) | | Tensile Strength (MPa) | Yield Strength Rp0.2, (%) | Elongation at Break, % | Modulus of Elasticity, (GPa) | Hardness (HRC) * |
|---|---|---|---|---|---|---|
| direction<br>8.0–8.1<br>direction | (a) | XY<br>1000–1200<br>Z | XY<br>1950–1150<br>Z | XY<br>6–14<br>Z | XY<br>135–185<br>Z | 33–37 |
| 8.0–8.1 | (a) | 1000–1200 | 1850–1150 | - | 130–170 | |
| | (b) | 1950–2150 | 1090–1290 | 2–6 | | 50–56 |

* Hardness measured on polished surface.

**Table 4.** Thermal Properties of Parts recommended by the manufacturer.

| | As Built | Hardened * |
|---|---|---|
| Thermal conductivity | 14.2–15.8 W/m °C | 19–21 W/m °C |
| Specific heat capacity | 430–470 J/kg °C | |
| Operating temp. | max. 400 °C | |

* Hardened temperature at 490 °C/ 6 h, cooling on the air.

### *2.1. Experiment Preparation*

The samples were produced on additive manufacturing machine by the EOSINT company, with the designation EOSINT M280, intended for additive manufacturing of metal products. This 3D printer has 250 × 250 × 325 mm volume of chamber. This type employs the Yb fiber laser with a maximum 400 W beam power, up to 700 mms$^{-1}$ scan speed, and 80 µm focus diameter. EOS Maraging Steel MS1 was used for the sample preparation. A shape and a size of the input powder material MS1 is plotted in Figure 4. A powder was observed using the scanning electron microscope SEM f. Tescan type Mira 3 and chemical composition was evaluated using the EDX analyser f. Oxford. A various size of spherically shaped particles can be observed. Experimental powders, evaluated using the spectral EDX analysis (Figure 4b), showed values corresponding to the values of the manufacturer, in a wider spectrum (Table 2).

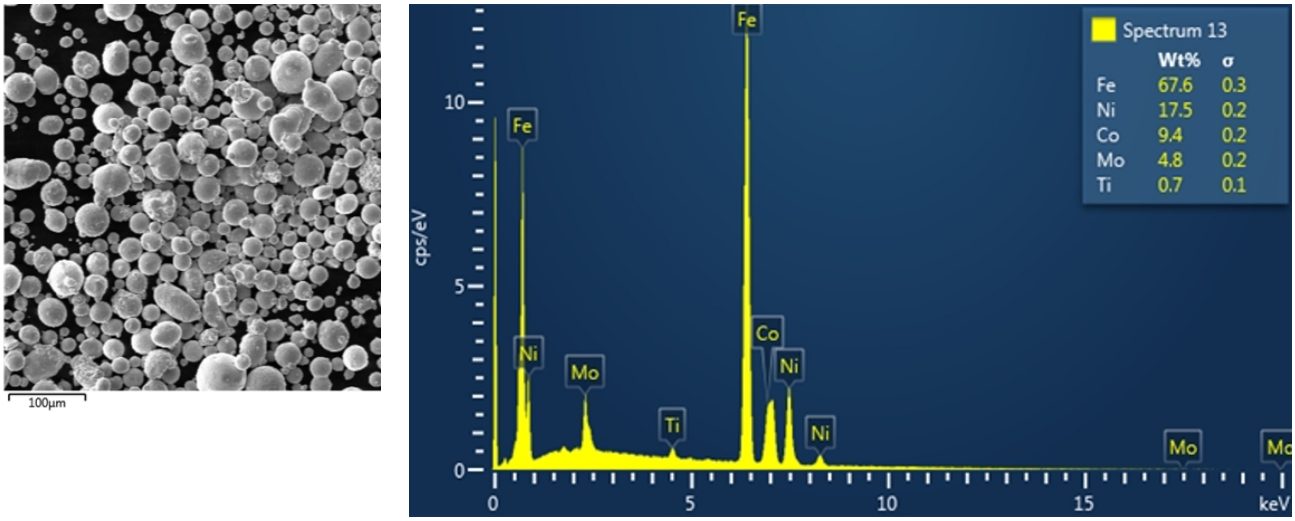


**(a)** **(b)**

**Figure 4.** A shape and a size of powder material MS1, evaluated using SEM Tescan Mira 3 (**a**), EDX analysis of powder, using f. Oxford analyzer (**b**).

EOSINT M280 AM system is able to print the component, based on the. stl file, straight from the CAD designs. For melting the powder, the laser power was adjusted to 200 W, the scanning speed to 650 mms$^{-1}$ and the hatching distance to 80 µm. Layer thickness was set on 40 µm for the layering process, and throughout the PBF process, the whole printing system was shielded by argon (Ar) gas. Meander printing strategy, with 100% infill setting, was used. Dimensions of tested samples were (XxZxY) 10 × 10 × 30mm. Dimensions and a shape of the material during printing, are shown in Figure 5. The layering of the material, during the DMLS process, was in the direction of the Z axis.

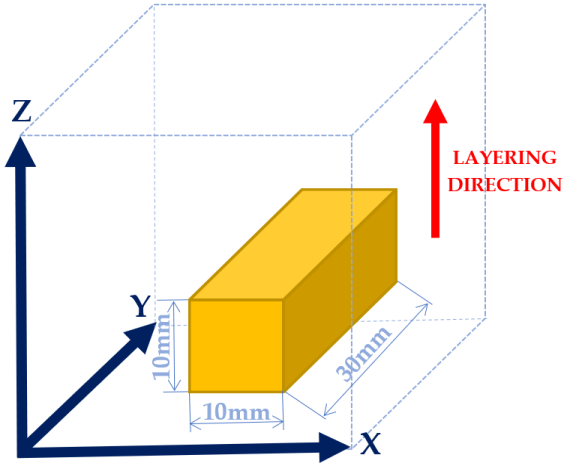


**Figure 5.** Scheme of the principle of DMLS printing for structure creation.

### *2.2. Process of Thermal Treatment*

Heat treatment by aging (age hardening) took place in the LAC device (Figure 6). The LAC device is an electric induction furnace with the possibility of setting temperature profiles. The chosen temperature profile was from a room temperature of 20 °C to a curing temperature of 590 °C in 30 min and maintaining at a temperature of 590 °C for the entire experiment for 6 h. The raising to the curing temperature was monitored using a FLIR T1030SC thermal camera (Figure 7).


**Figure 6.** Induction furnace LAC.

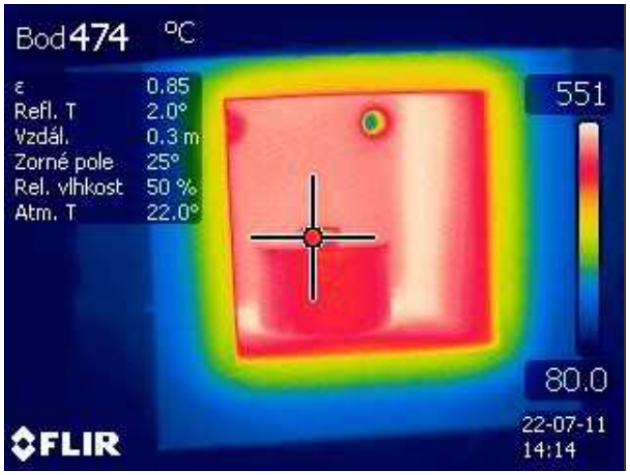


**Figure 7.** Verification of the raising temperature using a FLIR T1030SC thermal camera.

Prepared samples of the investigated material were gradually hardened in an induction furnace with an initial run-up time of 30 min. to a temperature of 590 °C. After the duration of 1, 2, 3, 4, 5 and 6 h, were taken out on a concrete pad and cooled in the still air, at a room temperature of 20 °C. To compare the effect of cooling in the air and cooling in the furnace, samples prepared at 2 and 6 h were cooled differently. One was cooled in the turned off furnace and the other was removed and cooled in the still air.

### *2.3. Preparation of Samples for Microstructure Observation and Hardness Evaluation*

Selected places for the evaluation of hardness and microstructure were chosen in the center of the sample, in the cross section of the x-z axis and the x-y axis, in order to observe the effect of heat treatment inside the material. The observed locations are marked in Figure 8. Material samples after heat treatment were split by abrasive water jet (AWJ) technology. AWJ technology is suitable for cutting of samples, because it does not thermally affect the material [40]. Samples for microstructure observation were prepared by grinding on the f. MTH Hrazdil device with the help of water cooling, sandpapers with grits of 180,

320, 500, 1200, 2000 and 4000. Then, samples were polished on a satin cloth with applied diamond polishing paste 0.1 µm.

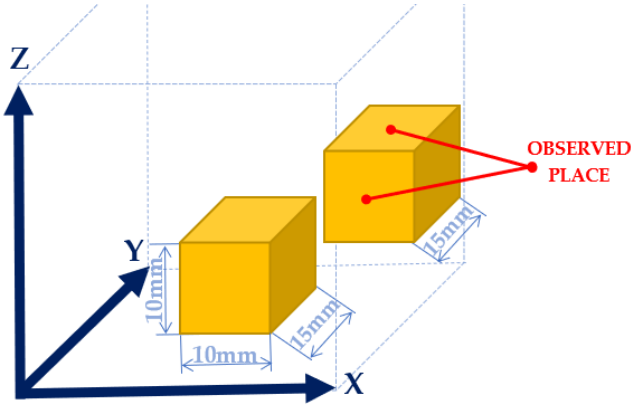


**Figure 8.** Section of material samples after temp. processing with a marked point of evaluation of hardness and microstructure.

The material samples were then observed with a Nikon MA100 light microscope and evaluated on Rockwell Insize ISH-RSR400 hardness testers. Cooling temperature was measured with thermal camera FlirT1030SC.

## 3. Results and Discussion

Measured cooling temperature dependences of MS1 material samples after heat treatment at a temperature of 590 °C, taken from the induction furnace after 1, 2, 3, 4 and 6 h, were cooled in the still air at a room temperature of 20 °C. Observation of the cooling process lasted approximately 20–30 min. Temperature was measured with thermal camera (Figure 9). Figure 10 shows the temperature dependence of the sample that was cooled in the furnace.

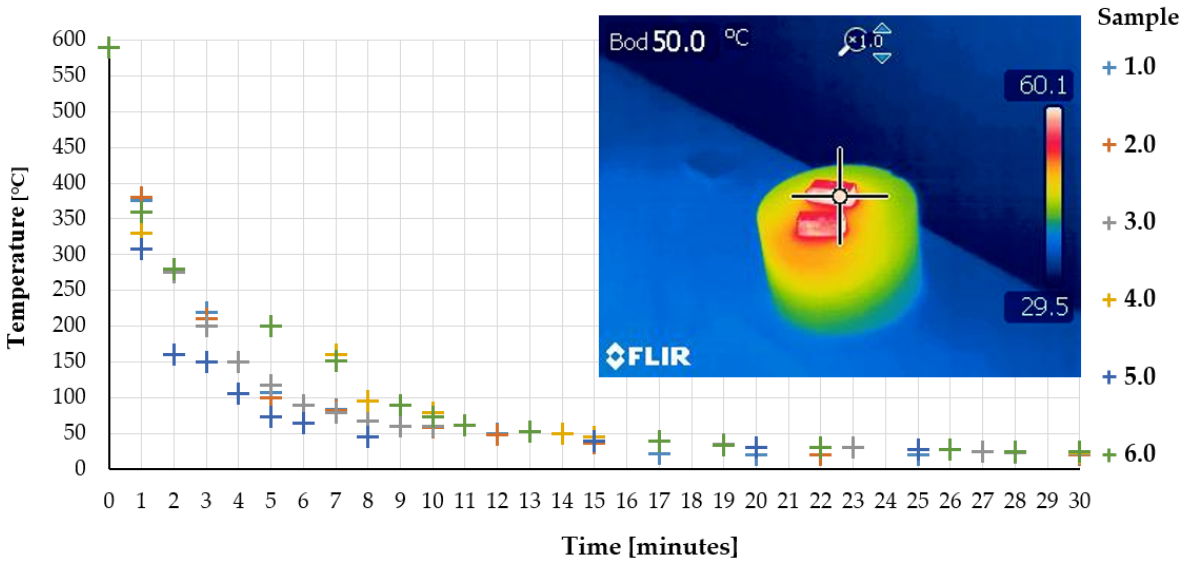


**Figure 9.** Temperature curve of cooling in the still air.

Tables below show Rockwell hardness measurements on samples with different lengths of used heat treatment process. Table 5 shows the hardness measurement at the center of the sample surface on each side. Table 6 shows the hardness measurement in the cross section of the sample. Sample 0.0 is shown for comparison, printed only,

without heat treatment. The first sample number is the duration value, e.g., 1.0—length of maintaining at a temperature for 1 h.

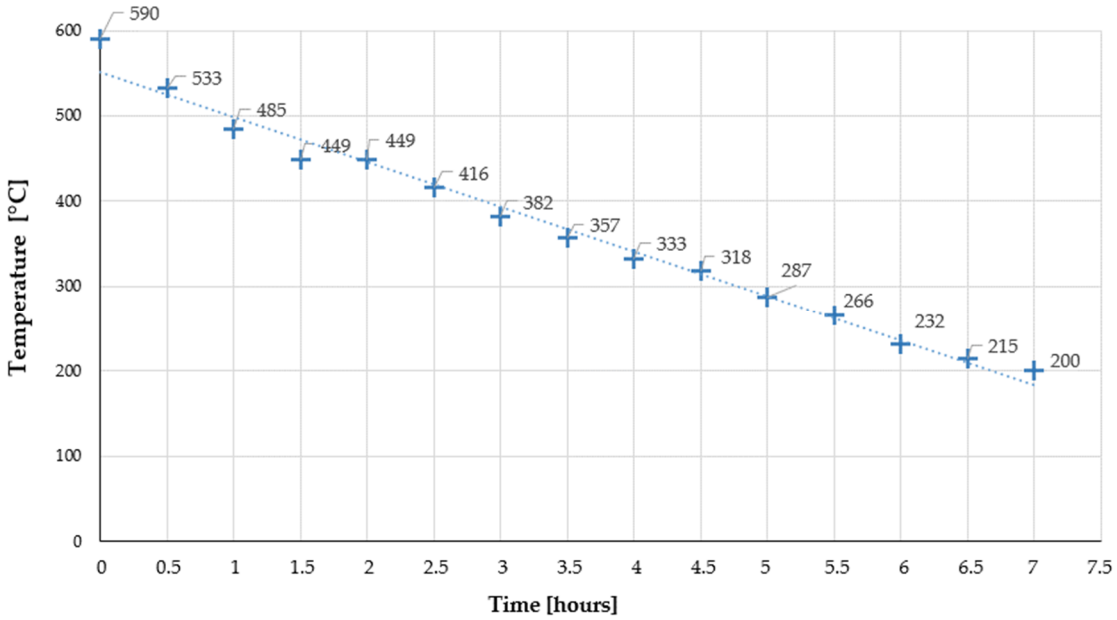


**Figure 10.** Temperature curve of cooling in the furnace.

**Table 5.** Rockwell hardness measurement values at the center of the sample surface.

| Sample | Measuring Side, Hardness Value | | | | Average Hardness Value |
|---|---|---|---|---|---|
| | x-y(Bottom) | x-y(Top) | y-z(Right Side) | y-z(Left Side) | |
| 0.0 * | 36.7 | | | | 36.7 |
| 1.0 | 29.6 | 50.4 | 47.8 | 47.9 | 43.9 |
| 2.0 | 27.1 | 48.1 | 36.7 | 45.2 | 39.3 |
| 2.1 ** | 35.1 | 45.9 | 37.9 | 48.8 | 41.9 |
| 3.0 | 40.5 | 37.9 | 42.4 | 41.1 | 40.5 |
| 4.0 | 25.1 | 37.3 | 46.4 | 45.7 | 38.6 |
| 5.0 | 32.5 | 46.3 | 37.5 | 47 | 40.8 |
| 6.0 | 37 | 51.3 | 42.7 | 45.8 | 44.2 |
| 6.1 ** | 21.9 | 42.7 | 49.8 | 46.8 | 40.3 |

*—only printed, without heat treatment. **—after cooling in furnace.

Hardness values after different lengths of stay at the tested temperature of 590 °C in all cases compared to only printed samples showed a higher hardness. Even after 1 h of holding at the temperature, average hardness was 44 HRC and in the cut surface 51 HRC. The lower value for these samples was distorted by the measurement at the bottom of the sample, where can be assumed that the surface of the construction platform is still insufficiently sanded. This artifact appears in every sample where the hardness values are clearly lower. During the measurement in the cut surface, this phenomenon did not occur, as we performed the measurement about 1 mm below the surface. With a longer duration for 2, 3, 4, 5 and 6 h, the hardness values decreased slightly. In the experimental evaluation of cooling in the still air—marked samples 2.0 and 6.0 and in the furnace—samples marked 2.1 and 6.1, these showed a slight increase in hardness only on the surface. The center of the sample did not change or slightly decreased. Therefore, can be assumed that the most ideal time for increasing the hardening temperature from 490 °C to 590 °C is 1 h and free cooling in the air.

**Table 6.** Rockwell hardness measurement values in the cross section of the sample.

| Sample | Measuring Side, Hardness Value | | | | Average Hardness Value | Measurement in the Center |
|---|---|---|---|---|---|---|
| | x-z (Bottom) | x-z (Top) | x-z (Right Side) | x-z (Left Side) | | |
| 1.0 | 49.7 | 50.2 | 51 | 50.7 | 50.4 | 51 |
| 2.0 | 48.9 | 48.2 | 49.1 | 43.4 | 47.4 | 49.2 |
| 2.1 ** | 49.4 | 49.9 | 50.2 | 49.5 | 49.8 | 49.5 |
| 3.0 | 49.2 | 46.5 | 48.6 | 48.1 | 48.1 | 49.5 |
| 4.0 | 48 | 45.2 | 47.7 | 46.9 | 47 | 47.7 |
| 5.0 | 44.1 | 46 | 45.9 | 45.4 | 45.4 | 46.9 |
| 6.0 | 46.8 | 47.5 | 46.8 | 45.4 | 46.6 | 47.5 |
| 6.1 ** | 47 | 46.7 | 46 | 46 | 46.4 | 46.8 |

**—after cooling in furnace.

The following Figure 11 shows observed microstructures of samples before heat treatment in the x-z and x-y planes The microstructure in the y-z plane was similar to that in the x-z plane as these are cross-sectional planes. In the x-y plane, the trace after the laser melting of the particles is visibly larger compared to x-z and y-z. This is due to the longer trace of the laser beam movement. At both X-Z and X-Y planes, features characteristic for DMLS 3D printing technology were observed. In the evaluated planes, direction and shape of the laser layering, were observed. Additionally, individual layers during sintering of the material at the uniform distance of about 0.1 µm, equal to the laser displacement, can be observed.

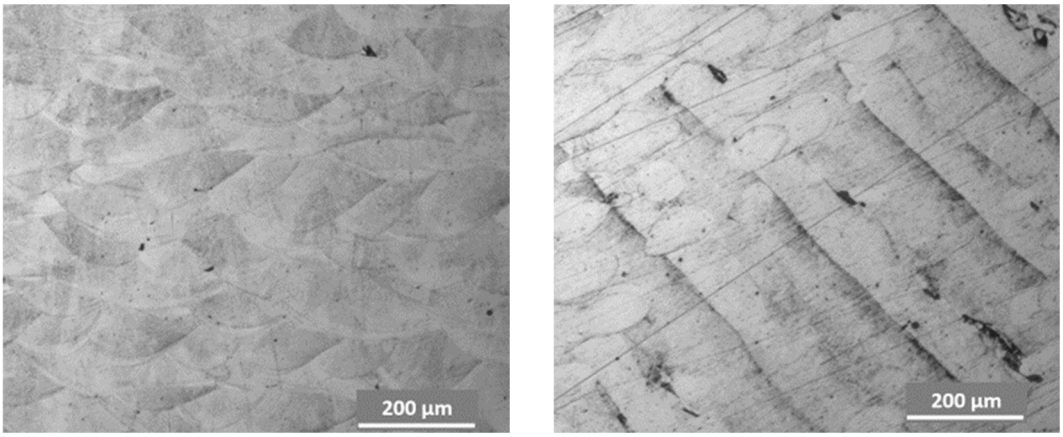


(**a**) (**b**)

**Figure 11.** Microstructure of sample without hardening process, only printed (sample 0.0), x-z plane (**a**), x-y plane (**b**), 100× magnification.

Observed microstructures of the MS1 material after heat treatment (Figures 12–14), showed similar layered formations typical of 3D printed samples. The microstructure of all heat-treated samples was uniform throughout the sample cross section. At a higher magnification of 1000x, a similar detail of the remelted particle with fine carbides can be seen again, with places of martensite lamellae. The microstructure at 1 and 2 h showed fine lamellae after the heat treatment, but not uniformly distributed, compared to the longer time of the heat process. At the 5 and 6 h interval, microstructures were quite similar and evenly distributed. In the 6 h interval of heat treatment, these lamellae are significantly softer, which is also indicated by the resulting hardness, which no longer increased rapidly. On the contrary, it was lower.

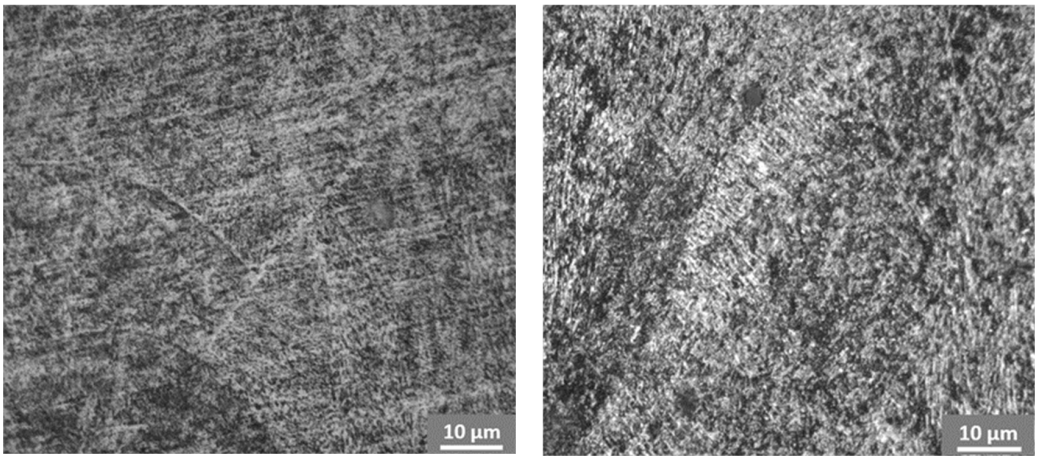


(**a**) (**b**)

**Figure 12.** Microstructure of the sample 1 h stay at 590 °C (sample 1.0) 1000× magnification (**a**); sample with length 2 h stay at 590 °C (sample 2.0) 1000× magnification (**b**).

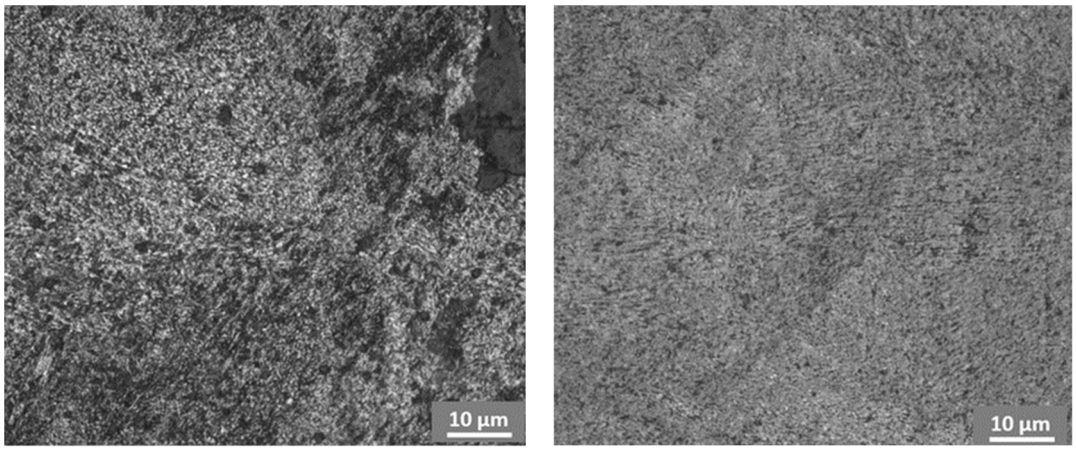


(**a**) (**b**)

**Figure 13.** Microstructure of the sample 3 h stay at 590 °C (sample 3.0) 1000× magnification (**a**); sample with length 4 h stay at 590 °C (sample 4.0) 1000× magnification (**b**).

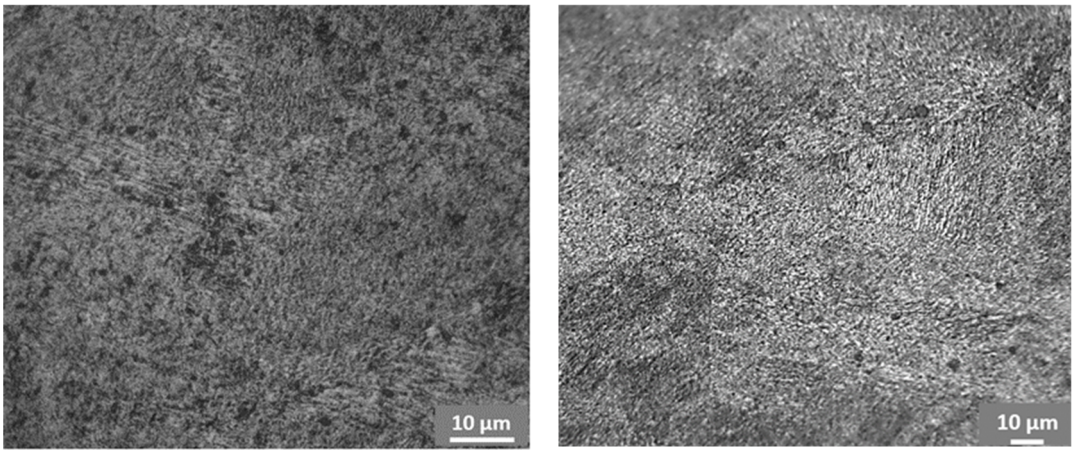


(**a**) (**b**)

**Figure 14.** Microstructure of the sample 5 h stay at 590 °C (sample 5.0) 1000× magnification (**a**); sample with length 6 h stay at 590 °C (sample 6.0) 500× magnification (**b**).

## 4. Conclusions

The article summarized the following claims:

Used heat treatment had an effect on pointing to a change in the length of stay at a temperature of 590 °C. The maintaining time proved to be the most ideal already at 1 h exposure and cooled in the still air, where a higher hardness value of around 50 HRC was reached. A longer maintaining time at 590 °C had the same or a slight decrease in hardness values. The manufacturer indicates a residence time for 6 h, at a temperature of 490 °C, where the values are around the level of 50 HRC. The microstructural evaluation was typical for the heat treatment, where fine carbides and martensitic lamellae were observed with a slight increase in hardness values in the microstructure. A more uniform and finer lamellar microstructure was shown with a longer interval of temperature exposure at 5 and 6 h intervals. This also indicates that the resulting hardness, which no longer increased rapidly, on the contrary, was somewhat lower, indicating a more relaxed state of the material after the hardening process.

**Author Contributions:** Conceptualization, V.S. and R.V.; investigation, R.V. and V.S.; data curation, R.V. and M.G.; original writing draft preparation, R.V. and V.S.; review writing and editing, V.S., R.V. and M.G.; visualization, Z.M.; supervision, V.S. and M.H. All authors have read and agreed to the published version of the manuscript.

**Funding:** This research was funded by the grant projects: KEGA no. 018TUKE-4/2021, VEGA 1/0391/22, APVV-21-0228 and ITMS no. 313011BWN5.

**Data Availability Statement:** Not applicable.

**Acknowledgments:** This work was funded by the Slovak Research and Development Agency under contract No APVV-21-0228 and the projects VEGA1/0391/22, KEGA 018TUKE-4/2021 were granted by the Ministry of Education, Science, Research and Sport of the Slovak Republic and this publication is the result of the Project implementation: Development of excellent research capacities in the field of additive technologies for the Industry of the 21st century, ITMS: 313011BWN5, supported by the Operational Program Integrated Infrastructure funded by the ERDF.

**Conflicts of Interest:** The authors declare no conflict of interest. The founding sponsors had no role in study design; when collecting, analyzing, or interpreting data; while writing the manuscript; or in the decision on the publication of the results.

## References

1. Mançanares, C.G.; de S. Zancul, E.; Cavalcante da Silva, J.; Miguel, P.A.C. Additive manufacturing process selection based on parts selection criteria. *Int. J. Adv. Manuf. Technol.* **2015**, *80*, 1007–1014. [CrossRef]
2. Yasa, E.; Kruth, J.-P. Microstructural investigation of selective laser melting 316L stainless steel parts exposed to laser re-melting. *Procedia Eng.* **2011**, *19*, 389–395. [CrossRef]
3. Palermo, E. Laserové spekanie. Available online: https://www.livescience.com/38862-selective-laser-sintering.html (accessed on 8 August 2019).
4. Dobránsky, J.; Kočiško, M.; Baron, P.; Simkulet, V.; Běhálek, L.; Vojnová, E.; Nováková-Marcinčínová, L'. Evaluation of the Impact Energy of the Samples Produced by the Additive Manufacturing Technology. *Metalurgija* **2016**, *55*, 477–480.
5. Monková, K. *Some Aspects of DMLS Technology*; RISE Association: Houston, TX, USA, 2017; p. 117. ISBN 978-80-87670-23-1.
6. Mower, T.M.; Long, M.J. Mechanical behavior of additive manufactured, powder-bed laser-fused materials. *Mat. Sci. Eng. A* **2016**, *651*, 198–213. [CrossRef]
7. Brandl, E.; Leyens, C.; Palm, F.; Schoberth, A.; Onteniente, P. Wire instead of powder? Properties of additive manufactured Ti–6Al–4V for aerospace applications. In Proceedings of the Euro-uRapid International Conference on Rapid Prototyping, Rapid Tooling & Rapid Manufacturing, Berlin, Germany, 23–24 September 2008.
8. Facchini, L.; Magalini, E.; Robotti, P.; Molinari, A.; Höges, S.; Wissenbach, K. Ductility of a Ti–6Al–4V alloy produced by selective laser melting of pre-alloyed powders. *Rapid Prototyp. J.* **2010**, *16*, 450–459. [CrossRef]
9. Van Hooreweder, B.; Boonen, R.; Moens, D.; Kruth, J.-P.; Sas, P. On the determination of fatigue properties of Ti6Al4V produced by selective laser melting. In Proceedings of the 53rd AIAA/ASME Structures, Structural Dynamics and Materials Conference, Honolulu, HI, USA, 23–26 April 2012.
10. Liu, Q.; Elambasseril, J.; Sun, S.; Leary, M.; Brandt, M.; Sharp, P.K. The effect of manufacturing defects on the fatigue behavior of Ti–6Al–4V specimens fabricated using selective laser melting. *Adv. Mater. Res.* **2014**, *891–892*, 1519–1524. [CrossRef]

11. Radchenko, S.; Knapčíková, L.; Dupláková, D.; Hatala, M. Verifikácia mechanických vlastností kompozitných materiálov v klimakomore. *Strojárstvo/Strojírenství. Roč.* **2016**, *10*, 82. (accessed on 1 October 2016).
12. Shellabear, M.; Nyrhilä, O. DMLS—Development History and State of the Art. Available online: https://www.i3dmfg.com/wp-content/uploads/2015/07/History-of-DMLS.pdf (accessed on 15 December 2022).
13. Ciraud, P. Verfahren und Vorrichtung zur Herstellung beliebiger Gegenstände aus beliebigem schmelzbarem Material. German Patent Application DE 2263777, 28 December 1971.
14. Housholder, R. Molding Process. US Patent 4,247,508, 3 December 1979.
15. Metal Additive Manufacturing History. Available online: https://additive-manufacturing-report.com/technology/metal/metal-additive-manufacturing-history/ (accessed on 15 November 2019).
16. Hull, C. Method and Apparatus for Production of Three-Dimensional Objects by Stereolithography. US Patent 4,575,330, 8 August 1984.
17. Deckard, C. Method and Apparatus for Producing Parts by Selective Sintering. US Patent 4,863,538, 17 October 1986.
18. Nyrhilä, O.; Syrjälä, S. Manufacture of dimensionally precise pieces by sintering. Finnish Patent Finnish Patent 91725, 7 April 1989.
19. Gašpár, Š.; Paško, J. Analysis of influence of pressing speed, of melt temperature and of casting position in a mold upon ultimate tensile strength Rm of die casting from aluminium. In *Advanced Materials Research: 2nd International Conference on Manufacturing 2014, Singapore, 9–10 February 2014*; Springer: Berlin/Heidelberg, Germany, 2014; Volume 909, pp. 3–7. ISBN 978-303835059-0. ISSN 1022-6680.
20. Simkulet, V.; Gusak, O.; Zajac, J.; Parilák, Ľ.; Mitaľová, Z. Verifikácia procesu tepelného spracovania materiálu vyrobeného technológiou priameho spekania laserom. In *Automatizácia a riadenie v teórii a praxi: ARTEP 2018*; Technical University of Košice: Košice, Slovakia, 2018; pp. 1–7. ISBN 978-80-553-2914-7.
21. Monkova, K.; Monka, P.; Mandulak, D. Hardness and Surface Roughness Study of Steel Part Produced by Additive Technology. *DEStech Trans. Eng. Technol. Res* **2017**. [CrossRef] [PubMed]
22. Yu, N. Process Parameter Optimization for Direct Metal Laser Sintering (DMLS). Ph.D. Thesis, National University of Singapore, Singapore, 2005.
23. Maharjan, N.; Wu, N.; Zhou, W. Hardening Efficiency and Microstructural Changes during Laser Surface Hardening of 50CrMo4 Steel. *Metals* **2021**, *11*, 2015. [CrossRef]
24. Kučerová, L.; Zetková, I.; Jeníček, Š.; Burdová, K. Production of Hybrid Joints by Selective Laser Melting of Maraging Tool Steel 1.2709 on Conventionally Produced Parts of the Same Steel. *Materials* **2021**, *14*, 2105. [CrossRef] [PubMed]
25. Sarafan, S.; Wanjara, P.; Gholipour, J.; Bernier, F.; Osman, M.; Sikan, F.; Molavi-Zarandi, M.; Soost, J.; Brochu, M. Evaluation of Maraging Steel Produced Using Hybrid Additive/Subtractive Manufacturing. *J. Manuf. Mater. Process.* **2021**, *5*, 107. [CrossRef]
26. Wang, X.; Chou, K. Effect of support structures on Ti-6Al-4V overhang parts fabricated by powder bed fusion electron beam additivemanufacturing. *J. Mater. Process. Technol.* **2018**, *257*, 65–78. [CrossRef]
27. Gåård, A.; Krakhmalev, P.; Bergström, J. Microstructural characterization and wear behavior of (Fe,Ni)–TiC MMC prepared by DMLS. *J. Alloys Compd.* **2006**, *421*, 166–171. [CrossRef]
28. Živčák, J.; Nováková-Marcinčínová, E.; Nováková-Marcinčínová, Ľ.; Balint, T.; Puškár, M. Increasing Mechanical Properties of 3D Printed Samples by Direct Metal Laser Sintering Using Heat Treatment Process. *J. Mar. Sci. Eng.* **2021**, *9*, 821. [CrossRef]
29. Zhao, Z.-Y.; Li, L.; Bai, P.-K.; Jin, Y.; Wu, L.-Y.; Li, J.; Guan, R.-G.; Qu, H.-Q. The Heat Treatment Influence on the Microstructure and Hardness of TC4 Titanium Alloy Manufactured via Selective Laser Melting. *Materials* **2018**, *11*, 1318. [CrossRef] [PubMed]
30. Avanzini, A.; Battini, D.; Gelfi, M.; Girelli, L.; Petrogalli, C.; Pola, A.; Tocci, M. Investigation on fatigue strength of sand-blasted DMLS-AlSi10Mg alloy. *Procedia Struct. Integr.* **2019**, *18*, 119–128. [CrossRef]
31. Rafi, H.K.; Starr, T.L.; Stucker, B.E. A comparison of the tensile, fatigue and fracture behavior of Ti–6Al–4V and 15–5 PH stainless steel parts made by selective laser melting. *Int. J. Manuf. Technol.* **2013**, *69*, 1299–1309. [CrossRef]
32. Simm, T.H.; Sun, L.; Galvin, D.R.; Hill, P.; Rawson, M.; Birosca, S.; Gilbert, E.P.; Bhadeshia, H.; Perkins, K. The effect of a two-stage heat-treatment on the microstructural and mechanical properties of a maraging steel. *Materials* **2017**, *10*, 1346. [CrossRef] [PubMed]
33. Shamantha, C.R.; Narayanan, R.; Iyer, K.J.L.; Radhakrishnan, V.M.; Seshadri, S.K.; Sundararajan, S.; Sundaresan, S. Microstructural changes during welding and subsequent heat treatment of 18Ni (250-grade) maraging steel. *Mater. Sci. Eng. A* **2000**, *287*, 43–51. [CrossRef]
34. N'Dri, N.; Mindt, H.W.; Shula, B.; Megahed, M.; Peralta, A.; Kantzos, P.; Neumann, J. DMLS Process Modeling and Validation. In Proceedings of the TMS 2015 144th Annual Meeting & Exhibition, Orlando, FL, USA, 15–19 March 2015; pp. 389–396.
35. Sun, S.; Brandt, M.; Easton, M. Powder bed fusion processes: An overview. In *Laser Additive Manufacturing: Materials, Design, Technologies, and Applications*; Woodhead Publishing Series in Electronic and Optical Materials; Elsevier: Amsterdam, The Netherlands, 2017; pp. 55–77.
36. About Additive Manufacturing. Available online: https://www.lboro.ac.uk/research/amrg/about/the7categoriesofadditivemanufacturing/powderbedfusion/ (accessed on 22 December 2022).
37. Edwards, P.; Ramulu, M. Fatigue performance of selective laser melted Ti–6Al–4V. *Mater. Sci. Eng. A* **2014**, *598*, 327–337. [CrossRef]
38. Available online: https://www.scribd.com/document/479137808/EOS-MaragingSteel-MS1-en-pdf# (accessed on 15 September 2022).

39. Available online: https://www.advancedtek.com/wp-content/uploads/2021/09/EOS_materials_table_overview_M_en_WEB.pdf (accessed on 15 December 2022).
40. Lebar, A.; Junkar, M. Simulation of abrasive waterjet machining based on unit event features. *Proc. Inst. Mech. Eng. Part B J. Eng. Manuf.* **2003**, *217*, 699–703. [CrossRef]